Propagation of non-Gaussian voltage angle fluctuations in high-voltage power grids

Ph. Jacquod * **M. Tyloo** **

* DQMP, University of Geneva, CH-1211 Geneva, and
School of Engineering, University of Applied Sciences of Western
Switzerland, CH-1951 Sion.
** Theoretical Division, Los Alamos National Laboratory, Los Alamos,
NM, USA

Abstract: Recent measurements have reported non-Gaussian tails in the distribution of frequency data in electric power grids. Large frequency deviations may induce grid instabilities and it is therefore crucial to understand how noise disturbances with long, non-Gaussian tails propagate. Here, we investigate how fluctuations in power feed-in, characterized by non-zero cumulants of their distribution, propagate through high-voltage power grids. Unlike previous investigations which focused on the white-noise limit, we consider the limit of long noise correlation time, where power feed-in fluctuates over times longer than the inherent dynamical time scales of the grid - the relevant regime for large-scale, high-voltage distribution grids. We show that in this limit, the skewness and kurtosis of the power feed-in distribution propagate similarly as its variance, independently of the distribution of inertia. Non-Gaussianities from individual sources of noise therefore persist throughout the entire network. This finding is corroborated by numerical results on a realistic model of the synchronous grid of continental Europe.

Keywords: Frequency fluctuations in power grids, non-Gaussian noise propagation.

1. INTRODUCTION

Recent analyses of large frequency datasets have uncovered non-Gaussianities in the distribution of local frequency fluctuations in AC power grids (Haehne et al., 2019; Rydin Gorjão et al., 2020, 2021; Schäfer et al., 2018), with distributions exhibiting long tails and occasional large increments. The source of these large frequency deviations is often attributed to the presence of new renewable sources of energy (Milan et al., 2013; Haehne et al., 2019; Wolff et al., 2019) – exhibiting fluctuating and uncertain power productions, with reduced electromechanical inertia (Machowski et al., 2008; Ulbig et al., 2014) – though the lack of data predating the rise of new renewables makes it difficult to confirm that conjecture directly. Large frequency deviations are an important risk factor for the safety of operation of AC electric power systems. It is therefore crucial to understand how non-Gaussian disturbances propagate through electric power networks. Many papers have investigated the propagation of disturbances originating from noisy power feed-in into power grids. For a necessarily incomplete list, the reader is referred to (Siami and Motee, 2016; Kettemann, 2016; Haehne et al., 2019; Tyloo et al., 2019; Pagnier and Jacquod, 2019b; Tumash et al., 2019; Wolff et al., 2019; Schröder et al., 2020). Most of these investigations focused on white Gaussian noise, with few notable exceptions. Based on numerical simulations, (Haehne et al., 2019) conjectured that the variance of frequency fluctuations decays faster as a function of the

distance to its source than its kurtosis. A similar effect has been furthermore reported in (Wolff et al., 2019), where non-Gaussianities seemed to be amplified in certain electric networks. Different noise probability distributions have been investigated, however time-uncorrelated white-noises have been considered almost systematically. White-noise distributions correspond to the limit of noise fluctuating over a time scale shorter than all other time scales characterizing the system. Recent analysis have however concluded that damping and network-dynamical time scales do not exceed few seconds in large-scale AC power grids (Tyloo et al., 2019; Pagnier and Jacquod, 2019b), therefore, the relevant limit for significant, persistent power feed-in fluctuations is the opposite limite of long noise correlation times. This motivates us to go beyond the white-noise regime.

In this manuscript, we investigate the propagation of voltage angle waves induced by Gaussian and non-Gaussian noise disturbances with long correlation time, through large-scale meshed power grids. The short-time voltage angle dynamics is commonly modelled by the swing equations (Machowski et al., 2008). Fluctuating power feed-in, generate waves that spread through the system. We model these fluctuations as noisy source terms, with a distribution characterized by its cumulants and a long correlation time τ_0. Given a source of non-Gaussian noise, we calculate the skewness and kurtosis of the voltage angle distributions at any node on the power grid, over the distribution of the power feed-in noise at a given location. We find that when τ_0 is the longest time scale,

these cumulants propagate throughout the power network just like the variance. Because non-vanishing cumulants correspond to deviations from Gaussianity, we conclude that non-Gaussian fluctuations of power feed-in with long correlation times propagate over the whole power grid. These analytical findings are corroborated by numerical simulations on a realistic model of the synchronous grid of continental Europe.

2. MATHEMATICAL NOTATION

We write vectors as $\boldsymbol{v} \in \mathbb{R}^n$, matrices as $\boldsymbol{M} \in \mathbb{R}^{n \times n}$, and diagonal matrices made of vector components as $\operatorname{diag}(\{v_i\})$.

The power networks are modeled as undirected weighted graphs $\mathcal{G} = (\mathcal{N}, \mathcal{E}, \mathcal{B})$ where $\mathcal{N}$ is the set of its n nodes/vertices, $\mathcal{E}$ is the set of edges, and $\mathcal{B} = \{B_{ij} > 0\}$ is the set of edge weights, corresponding to line susceptances between connected nodes i and j. The graph Laplacian $\boldsymbol{L}^{(0)} \in \mathbb{R}^{n \times n}$ is the symmetric matrix defined as $\boldsymbol{L}^{(0)} = \sum_{i<j} B_{ij} \boldsymbol{e}_{(i,j)} \boldsymbol{e}_{(i,j)}^\top$, with $\boldsymbol{e}_{(i,j)} = \boldsymbol{e}_i - \boldsymbol{e}_j$ in terms of the unit vector $\boldsymbol{e}_i \in \mathbb{R}^n$ whose components read $(e_i)_l = \delta_{il}$, with the Kronecker δ. The graph Laplacian has eigenvalues $\{\lambda_1, \ldots \lambda_n\}$ corresponding to an orthonormal basis of eigenvectors $\{\boldsymbol{u}_1, \ldots, \boldsymbol{u}_n\}$. The zero row and column sum property of $\boldsymbol{L}^{(0)}$ implies that $\lambda_1 = 0$ and that $\boldsymbol{u}_1^\top = (1, \ldots, 1)/\sqrt{n}$. In connected graphs, $\lambda_\alpha > 0$ for $\alpha = 2, \ldots, n$. A weighted Laplacian matrix $\boldsymbol{L}$ will be considered below [see Eq. (2)], where the edge weights are normalized by the cosine of voltage angle differences at the corresponding nodes, defined by the operational steady-state of the grid.

The effective resistance distance between any two nodes i and j of the network is defined as $\Omega_{ij} = \boldsymbol{e}_{(i,j)}^\top \boldsymbol{L}^\dagger \boldsymbol{e}_{(i,j)}$, with the Moore-Penrose pseudoinverse $\boldsymbol{L}^\dagger$ of the graph Laplacian matrix (Klein and Randić, 1993; Stephenson and Zelen, 1989). This quantity is a graph theoretical distance metric satisfying the properties: i) $\Omega_{ii} = 0 \; \forall i$, ii) $\Omega_{ij} \geq 0 \; \forall i \neq j$, and iii) $\Omega_{ij} \leq \Omega_{ik} + \Omega_{kj} \; \forall i, j, k$. It is known as the *resistance* distance because if one replaces each edge (k, l) of $\mathcal{G}$ by a resistor with a conductance $1/R_{kl} = B_{kl}$, then Ω_{ij} is equal to the equivalent network resistance when a current is injected at node i and extracted at node j with no injection anywhere else. The resistance distance can be written $\Omega_{ij} = \sum_{\alpha \geq 2} \lambda_\alpha^{-1} (u_{\alpha,i} - u_{\alpha,j})^2$, in terms of the eigenvalues and eigenvectors of $\boldsymbol{L}$ (Klein, 1997; Xiao and Gutman, 2003).

The average resistance distance between a given node i and all the other nodes in the network define the resistance centrality $C_1(i) = (n^{-1} \sum_j \Omega_{ij})^{-1}$ of node i, and the average resistance distance over all pairs of nodes give the resistance graph efficiency also called the Kirchhoff index, $Kf_1 = \sum_{i<j} \Omega_{i,j}$ (Klein and Randić, 1993; Stephenson and Zelen, 1989).

We will consider noisy disturbances in the form of fluctuating power feed-in $\delta\boldsymbol{p}(t)$. The probability distribution of the latter defines an ensemble over which we calculate averages, denoted by $\langle \ldots \rangle$. We differentiate moments, $\langle \delta\theta_i^p \rangle$, and cumulants, $\langle \delta\theta_i^p \rangle_c$, of the distribution of voltage angles.

3. DYNAMICS OF AC POWER GRIDS

We consider the voltage angle and frequency dynamics of a high voltage AC power network in the lossless, DC power flow approximation. This standard approximation assumes uniform and constant voltage amplitude, non-resistive power transmission lines and small voltage angle differences. The stationary power flow equations $\boldsymbol{p}^{(0)} = \boldsymbol{L}^{(0)} \boldsymbol{\theta}^{(0)}$ relates the vector of active power injections $\boldsymbol{p}^{(0)}$ to the vector of voltage angles $\boldsymbol{\theta}^{(0)}$ in the operational stationary state. The Laplacian matrix $\boldsymbol{L}^{(0)}$ of the graph represents the electric power grid, i.e. its nonzero matrix elements are given by minus the susceptance B_{ij} of the transmission lines between connected nodes i and j.

Dynamical effects set in when the system is brought out of equilibrium by some disturbance. Here we consider a time-dependent power feed-in perturbation $\boldsymbol{p}(t) = \boldsymbol{p}^{(0)} + \delta\boldsymbol{p}(t)$, which locally perturbs the balance between the mechanical torque supplied by the rotating machine and the electrical torque output of the alternator. Under the assumption that each network node has a synchronous machine (generator or consumer) of rotational inertia $m_i > 0$ and damping coefficient $d_i > 0$, and assuming that the disturbance is weak enough that it primarily affects voltage angles and not their amplitudes, the network dynamics is governed by the swing equations (Machowski et al., 2008). In the frame rotating at the nominal frequency of the network, and under the just mentioned assumptions, they read

$$\boldsymbol{M} \delta\ddot{\boldsymbol{\theta}} = -\boldsymbol{D} \delta\dot{\boldsymbol{\theta}} + \delta\boldsymbol{p}(t) - \boldsymbol{L} \delta\boldsymbol{\theta}, \qquad (1)$$

with $\boldsymbol{\theta}(t) = \boldsymbol{\theta}_i^{(0)} + \delta\boldsymbol{\theta}(t)$, $\boldsymbol{M} = \operatorname{diag}(\{m_i\})$ and $\boldsymbol{D} = \operatorname{diag}(\{d_i\})$, and the weigthed Laplacian matrix

$$\mathbf{L}_{ij} = \begin{cases} -B_{ij} \cos(\theta_i^{(0)} - \theta_j^{(0)}), & \text{for } i \neq j, \\ \sum_k B_{ik} \cos(\theta_i^{(0)} - \theta_j^{(0)}), & \text{for } i = j. \end{cases} \qquad (2)$$

Eq. (1) describes the small-signal stability problem Machowski et al. (2008), on which we focus.

4. MODAL DECOMPOSITION

Eq. (1) is a linear differential equation that governs the propagation of the local disturbance modeled by a time-dependent source term $\delta\boldsymbol{p}(t)$. The Laplacian matrix $\boldsymbol{L}$ replaces the Laplace operator of continuous wave equations. It encodes a discrete, meshed complex power network defined between load and generator nodes. Load nodes in principle have $m_i = 0$ and a damping parameter d_i significantly smaller than generators. However, it is possible to Kron-reduce the network (Kron, 1939) into an effective network with modified line susceptances connecting only inertiaful, generator nodes. This transformation is based on Schur's complement formula (Horn and Johnson, 1986), and since the reduced load nodes have no inertia and a much smaller damping term, this reduction modifies the dynamics on the generators only marginally. In our analytical treatment, we will consider noise propagation from Eq. (1) for a Kron-reduced network. An approximation we make in our analytical treatment, but not in our numerics, is that damping and inertia are uniform, $d_i = d$, $m_i = m$. This is a standard assumption when analytically calculating voltage angle and frequency deviations (Tegling et al., 2015; Paganini and Mallada, 2017; Poolla et al., 2017;

Grunberg and Gayme, 2018; Pagnier and Jacquod, 2019a). Below, we validate our analytical results with numerical simulations not relying on this homogeneity assumption.

We want to compute the moments $\mu_p = \langle \delta\theta_i^p \rangle$, $p \leq 4$ of the distribution of angle deviations at any node on the network and relate them to the statistical properties of the noisy source term. We perform a modal expansion of the voltage angles over the eigenmodes $\{\mathbf{u}_\alpha\}$ of $\boldsymbol{L}$, $\delta\boldsymbol{\theta}(t) = \sum_\alpha c_\alpha(t)\,\mathbf{u}_\alpha$, to obtain

$$m\,\ddot{c}_\alpha + d\,\dot{c}_\alpha + \lambda_\alpha c_\alpha = \delta\boldsymbol{p}(t)\cdot\mathbf{u}_\alpha\,, \tag{3}$$

where $\boldsymbol{L}\mathbf{u}_\alpha = \lambda_\alpha\mathbf{u}_\alpha$, with $\lambda_\alpha \geq 0$, $\alpha = 1,\dots N$. Eq. (3) is a differential equation for a damped, driven harmonic oscillator. We solve it using Laplace transforms to obtain (Tyloo and Jacquod, 2019)

$$c_\alpha(t) = m^{-1}e^{-(\gamma+\Gamma_\alpha)t/2}\int_0^t e^{\Gamma_\alpha t_2}$$
$$\times\int_0^{t_2} e^{(\gamma-\Gamma_\alpha)t_1/2}\,\delta\boldsymbol{p}(t_1)\cdot\mathbf{u}_\alpha\,\mathrm{d}t_1\mathrm{d}t_2\,, \tag{4}$$

with $\Gamma_\alpha = \sqrt{\gamma^2 - 4\lambda_\alpha/m}$ and $\gamma = d/m$. From Eq. (4), the pth voltage angle moment μ_p contains an average $\langle \delta p_{i_1}(t_1)\delta p_{i_2}(t_2)\dots\delta p_{i_p}(t_p)\rangle$, over the product of p sources of noise, inside exponential integrals. We calculate μ_p assuming zero-average feed-in noise at node i_0 in the network. Specifically, the first two moments are given by

$$\langle \delta p_i(t_1)\rangle = 0\,, \tag{5a}$$
$$\langle \delta p_i(t_1)\delta p_j(t_2)\rangle = \sigma^2\,\delta_{ij}\delta_{ii_0}e^{-|t_1-t_2|/\tau_0}\,. \tag{5b}$$

This defines the noise correlation time τ_0, which we take as the largest time-scale. To take non-Gaussianities into account, we further consider finite skewness and kurtosis of the noise distribution as

$$\langle \delta p_i(t_1)\delta p_j(t_2)\delta p_k(t_3)\rangle = a_3\,\sigma^3\,\Delta_{ijk}\delta_{ii_0}\,, \tag{6a}$$
$$\langle \delta p_i(t_1)\delta p_j(t_2)\delta p_k(t_3)\delta p_l(t_4)\rangle_c = a_4\,\sigma^4\,\Delta_{ijkl}\delta_{ii_0}\,, \tag{6b}$$

where the long correlation time limit has already been considered to shorten the notation, $\Delta_{ijk}\neq 0$ for $i = j = k$ only (similarly for Δ_{ijkl}) and $\langle\dots\rangle_c$ explicitly refers to the cumulant, which in particular substracts all partial pairings such as $\langle \delta p_i(t_1)\delta p_j(t_2)\rangle\langle \delta p_k(t_3)\delta p_l(t_4)\rangle$. The parameters $a_{3,4}\neq 0$ characterize non-Gaussianities in the noise distribution. They correspond to skewed distributions ($a_3 \neq 0$), with longer tails ($a_4 > 0$) or both.

Eq. (3) makes it clear that, beside τ_0, the other time scales are the damping time $\gamma^{-1} = m/d$, the period $T_\alpha = \sqrt{m/\lambda_\alpha}$ of the αth oscillating mode and the combination $\gamma T_\alpha^2 = d/\lambda_\alpha$ of the two. For the synchronous grid of continental Europe, a time scale analysis found $\gamma^{-1} \simeq 2.5s$, $T_\alpha < 1s$ and $\gamma T_\alpha^2 < 0.4s\ \forall\alpha$, and the long correlation time regime is already reached for $\tau_0 \gtrsim 5-10s$ (Pagnier and Jacquod, 2019b; Tyloo et al., 2019). Corrective actions such as line disconnections and/or reconnections occur on much shorter time scales, however they do not repeat themselves more than few times. It is hard to imagine how any persistent noise source would oscillate on time scales shorter than at least few seconds, which justifies to consider the long correlation time limit.

5. VOLTAGE ANGLE VARIANCE AND HIGHER CUMULANTS

We calculate the variance, skewness and kurtosis of the voltage angle at any node i on the network, given a disturbed power feed-in at node i_0. With the modal expansion discussed above, the variance is given by $\langle\delta\theta_i^2(t)\rangle = \sum_{\alpha,\beta}\langle c_\alpha(t)c_\beta(t)\rangle u_{\alpha,i}u_{\beta,i}$, with $c_{\alpha,\beta}(t)$ given in Eq. (4). Similar expressions give the skewness and the kurtosis. The results are the sum of terms that decay exponentially with t as $\propto \exp[-\lambda_\alpha t], \exp[-t/\tau_0]$ and terms that are constant in time. We consider the limit of large observation times, where only the constant terms matter. Considering the long noise correlation time limit, $\tau_0 \gg \gamma^{-1}, T_\alpha, \gamma T_\alpha^2$ a straightforward though tedious calculation gives,

$$\lim_{\tau_0\to\infty}\langle\delta\theta_i^p\rangle_c = a_p\left(\sigma\sum_{\alpha\geq 2}\frac{u_{\alpha,i_0}u_{\alpha,i}}{\lambda_\alpha}\right)^p\,, \tag{7}$$

where we set $a_2 = 1$ to cast the cumulants in a single equation. The full calculation leading to Eq. (7) will be given elsewhere, as it is too long to fit in this paper. In the Appendix, we give it for inertialess Kuramoto oscillators.

The cumulants are given by the pth power of the Green's function for the linear operator $\boldsymbol{L}$, from the noise source i_0 to the observation node i. For optical or electronic waves propagating through disordered mesoscopic systems, such quantities decay as power laws with the distance between i_0 and i, when averaged over a relatively narrow but high-lying spectral interval (Akkermans and Montambaux, 2007). Eq. (7) instead corresponds to a "zero-energy" Green's function, indicating that fluctuations are transmitted by few low-lying, long-wavelength eigenmodes of $\boldsymbol{L}$. The most remarkable thing is that, from Eq. (7), standardized higher cumulants are given by $\langle\delta\theta_i^p\rangle_c/|\langle\delta\theta_i^2\rangle|^{p/2} = \pm a_p$ (with a possible minus sign for odd cumulants), regardless of the distance between the measured node and the noise source. This is our main result: non-Gaussian fluctuations originating from a single noise source with long correlation time propagate just as Gaussian fluctuations do, over the whole system. This result is in particular independent of inertia, in agreement with our earlier findings (Tyloo and Jacquod, 2021).

A second interesting result comes from the fact that the Green's function can be rewritten in terms of the effective resistance distance between i_0 and i and the resistance graph efficiency, a centrality corresponding to the average of the resistance distance over all pairs of nodes in the whole graph, a quantity sometimes called the Kirchhoff index (Klein and Randić, 1993; Stephenson and Zelen, 1989). A direct calculation gives (remember that $\sum_i u_{\alpha,i} = 0$ for the $\alpha \geq 2$ eigenmodes of $\boldsymbol{L}$, since they are orthogonal to the constant $\alpha = 1$ eigenmode)

$$\sum_{\alpha\geq 2}\frac{u_{\alpha,i_0}u_{\alpha,i}}{\lambda_\alpha} = \frac{C_1^{-1}(i_0) + C_1^{-1}(i) - \Omega_{i_0 i} - 2Kf_1/n^2}{2}\,. \tag{8}$$

where $\Omega_{i_0,i}$ is the resistance distance between node i_0 and i, $C_1(i) = (n^{-1}\sum_j \Omega_{ij})^{-1}$ is the resistance centrality of node i and $Kf_1 = \sum_{i<j}\Omega_{i,j}$ is the resistance graph efficiency/the Kirchhoff index. These three quantities are

all positive, therefore, together with Eq. (7), Eq. (8) means that the sign of the third cumulant is determined by the balance between the centralities of the input and measurement nodes on the one hand, and the resistance distance between them on the other hand. In particular, the skewness changes sign some distance away from The standardized third cumulant is therefore constant in magnitude all over the network, with however sign changes.
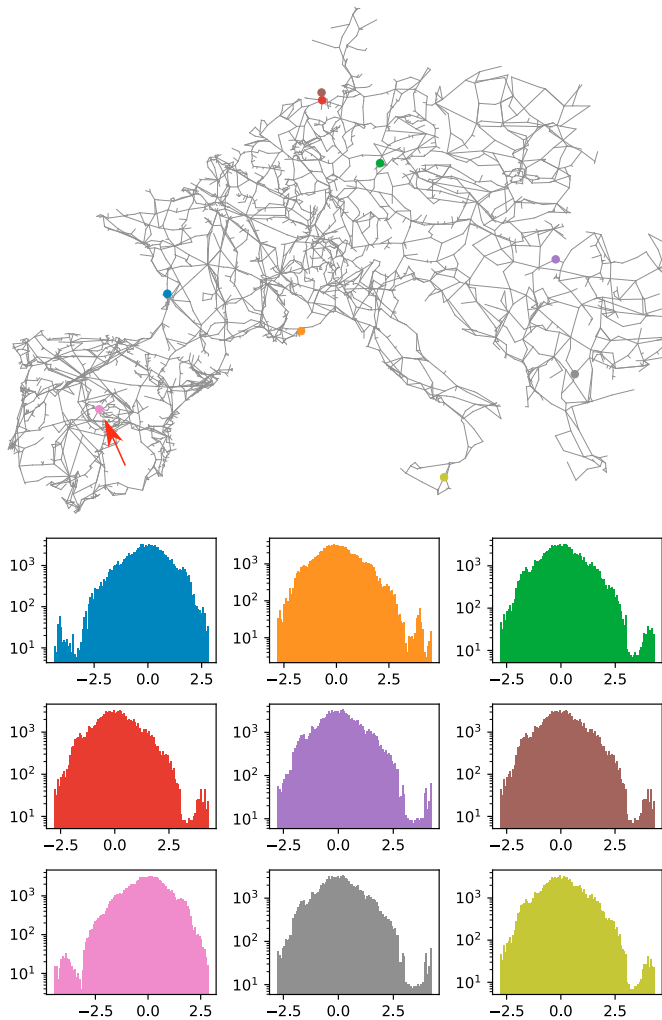

Fig. 1. Numerical simulation of Eq. (1) on the PanTa-GruEl model of the synchronous grid of continental Europe (Pagnier and Jacquod, 2019b; Tyloo et al., 2019) shown in the top panel. The disturbance is a non-Gaussian noisy signal injected at the node colored in pink and indicated by the red arrow. The nine histograms show the locally normalized distributions of angle deviation at the node with corresponding colors. The non-Gaussian asymmetry of the injected noise (see pink histogram) persists over the whole network, with a skewness inversion fully corroborating Eqs. (7) and (8).

6. NUMERICAL RESULTS

We confirm our analytical results with numerical simulations on PanTaGruEl, a realistic model of the very high voltage synchronous grid of continental Europe (Pagnier and Jacquod, 2019b; Tyloo et al., 2019). A map of the

model is shown in the top panel of Fig. 1. The model is not Kron-reduced. It is heterogeneous in the dynamical parameters m_i and d_i, in particular, load nodes have $m_i = 0$. Therefore, our numerical simulations test our analytical results in a realistic setting that is in particular not restricted by the above assumptions of constant inertia and damping. Eq. (1) is integrated, for a noisy disturbance located in Spain, and indicated on the map by a red arrow (pink node). The noisy disturbance has a non-Gaussian distribution whose histogram is shown in the pink histogram panel of Fig. 1. The fluctuations in angle voltages are recorded on eight other nodes, indicated by color dots in the model map. The normalized distributions of angle voltages at each of these nodes is shown in the histogram panels. The first, main observation is that these distributions are the same on all nodes, up to an inversion of the horizontal axis, $\delta\theta_i(t) \leftrightarrow -\delta\theta_i(t)$. That the shape of the distributions remain the same corroborates our result, Eq. (7), according to which the standardized cumulants are the same in absolute value on all nodes. Second, one sees that the voltage angle distribution on the blue node is the same as on the pink disturbance node, while all other measured distributions are left-right inverted, i.e. with $\delta\theta_i(t) \leftrightarrow -\delta\theta_i(t)$. This follows directly from Eq. (8). When i is very close to i_0, the sign of the odd cumulants is given by the sign of $C^{-1}(i_0) - Kf/n^2$. If i_0 is less central than the average node, as is the case for the chosen pink node in Fig. 1, that sign is positive, because $C^{-1}(i_0)$ is large for peripheral nodes, while Kf/n^2 is the average of $C^{-1}(i)$. When the distance between i and i_0 increases, so does the resistance distance $\Omega_{i_0,i}$ between disturbance and measurement, while simultaneously $C^{-1}(i)$ decreases. Eventually, this will change the sign of the Green's function in Eq. (8), and with it, the sign of all standardized odd cumulants. Note that the sign of these odd cumulants may already be negative when measurement and source nodes are close to one another, if i_0 lies in a central position on the network – when $C_1(i_0)$ is large. In that case, there is no sign change and the odd cumulants of the voltage angle deviations are negative all over the network.

7. CONCLUSION

We have reported on recent and preliminary investigations of non-Gaussian disturbance propagation in high-voltage AC power grids. The motivation is that deviations from Gaussian distributions have recently been observed in voltage angle and frequency distributions, and their origin remains an open question. In particular it remains to be understood whether the currently unfolding energy transition, with the associated substitution of traditional power generation with new renewable sources of energy will be accompanied by larger voltage angle and frequency deviations.

In this manuscript, we looked at how a local, non-Gaussian disturbance characterized by the cumulants of its probability distribution propagates across a large-scale meshed power grid. Our main contribution has been to identify a key ingredient that has so far been negected in similar investigations: the correlation time of the noisy disturbance, and its position with respect to other time scales in the system. We focused on a little explored regime where this correlation time is the largest time scale. Earlier time scale

analysis identify the regime of long correlation time as relevant for large-scale transmission grids, and we found that non-Gaussianities propagate similarly as Gaussian fluctuations. In particular, we showed analytically and confirmed numerically that for a single source of noise, all standardized cumulants of the voltage angle distribution are spatially constant, everywhere on the power network, regardless of the presence and distribution of the electro-mechanical inertia of traditional generators. This is important as it shows how a localized, non-Gaussian feed-in disturbance may persist, and actually perturb a large-scale power grid over long distances.

The next steps are, first to connect these results to the other limit of short correlation times, second to consider the superposition of several sources of noise, third to extend this investigation to the voltage frequency. Work along those lines is in progress and will be reported elsewhere.

Appendix A. CUMULANTS FOR KURAMOTO OSCILLATORS

The full calculation - including inertia - of our main analytical result, Eq. (7), is too long to fit in this size-restricted paper. Here we sketch the calculation of the voltage angle moments for inertialess oscillators corresponding to Eq. (1) with $m = 0$. We perform the modal expansion discussed in the main text, leading to Eq. (3), also with $m = 0$, whose solution reads

$$c_\alpha(t) = \exp[-\lambda_\alpha t] \int dt' \exp[\lambda_\alpha t'] \, \delta\mathbf{P}(t') \cdot \mathbf{u}_\alpha. \quad \text{(A.1)}$$

From the expansion $\delta\theta_i(t) = \sum c_\alpha(t)u_{\alpha i}$ of the voltage angle at site i over the ith component of the eigenmodes of $\boldsymbol{L}$, one obtains the pth moment of the voltage angle distribution $\langle \delta\theta_i^p(t) \rangle = \sum_{\alpha_1,...\alpha_p} \langle c_{\alpha_1}(t)...c_{\alpha_p}(t) \rangle u_{\alpha_1 i}...u_{\alpha_p i}$. From Eq. (A.1), these moments are therefore given by exponential integrals, once the noise moments of Eqs. (5) and (6) are inserted.

For the variance, one has

$$\langle c_\alpha(t)c_\beta(t) \rangle = \sum_{i_0,j_0} u_{\alpha,i_0} u_{\beta,j_0} \exp[-(\lambda_\alpha + \lambda_\beta)t] \quad \text{(A.2)}$$

$$\times \iint_0^t dt_1 dt_2 e^{\lambda_\alpha t_1 + \lambda_\beta t_2} \langle \delta P_{i_0}(t_1) \delta P_{j_0}(t_2) \rangle,$$

which, with Eq. (5b), gives

$$\langle \delta\theta_i^2(t) \rangle = 2\sigma^2 \tau_0^{-1} \sum_{\alpha,\beta} \frac{u_{\alpha\,i_0} u_{\beta\,i_0} u_{\alpha\,i} u_{\beta\,i}}{(\lambda_\alpha + \lambda_\beta)(\lambda_\alpha + \tau_0^{-1})(\lambda_\beta + \tau_0^{-1})}$$

$$+ \sigma^2 \sum_{\alpha,\beta} \frac{u_{\alpha\,i_0} u_{\beta\,i_0} u_{\alpha\,i} u_{\beta\,i}}{(\lambda_\alpha + \tau_0^{-1})(\lambda_\beta + \tau_0^{-1})}, \quad \text{(A.3)}$$

after two exponential integrals have been calculated. In the limit of long correlation times, Eq. (A.3) directly leads to Eq. (7) with $p = 2$.

Higher moments are calculated in the same way, which also leads to Eq. (7) in the limit of long correlation times. For the case with finite inertia, calculational steps are also the same, but are more complicated because of the doubling of the exponential integrals to be calculated from the expression (4) instead of (A.1). The resulting expression are lengthy, however, they also lead to Eq. (7) in the limit of long correlation time.

REFERENCES

Akkermans, E. and Montambaux, G. (2007). *Mesoscopic Physics of Electrons and Photons.* Cambridge University Press.

Grunberg, T.W. and Gayme, D.F. (2018). Performance measures for linear oscillator networks over arbitrary graphs. *IEEE Transactions on Control of Network Systems*, 5(1), 456–468.

Haehne, H., Schmietendorf, K., Tamrakar, S., Peinke, J., and Kettemann, S. (2019). Propagation of wind-power-induced fluctuations in power grids. *Phys. Rev. E*, 99, 050301.

Horn, R.A. and Johnson, C.R. (1986). *Matrix Analysis.* Cambridge University Press, New York.

Kettemann, S. (2016). Delocalization of disturbances and the stability of ac electricity grids. *Phys. Rev. E*, 94, 062311.

Klein, D.J. and Randić, M. (1993). Resistance distance. *J. Math. Chem.*, 12(1), 81–95.

Klein, D.J. (1997). Graph geometry, graph metrics and Wiener. *Commun. Math. Comput. Chem.*, 35, 7.

Kron, G. (1939). *Tensor Analysis of Networks.* Wiley.

Machowski, J., Bialek, J.W., and Bumby, J.R. (2008). *Power System Dynamics.* Wiley, Chichester, U.K, 2nd edition.

Milan, P., Wächter, M., and Peinke, J. (2013). Turbulent character of wind energy. *Phys. Rev. Lett.*, 110, 138701.

Paganini, F. and Mallada, E. (2017). Global performance metrics for synchronization of heterogeneously rated power systems: The role of machine models and inertia. *55th Annual Allerton Conference on Communication, Control, and Computing*, 324–331.

Pagnier, L. and Jacquod, P. (2019a). Optimal placement of inertia and primary control: A matrix perturbation theory approach. *IEEE Access*, 7, 145889.

Pagnier, L. and Jacquod, P. (2019b). Inertia location and slow network modes determine disturbance propagation in large-scale power grids. *PLoS ONE*, 14, 1–17.

Poolla, B.K., Bolognani, S., and Dörfler, F. (2017). Optimal Placement of Virtual Inertia in Power Grids. *IEEE Transaction Automatic Control*, 62(12), 6209–6220. doi: 10.1109/TAC.2017.2703302.

Rydin Gorjão, L., Jumar, R., Maass, H., Hagenmeyer, V., Yalcin, G., Kruse, J., Timme, M., Beck, C., Witthaut, D., and Schäfer, B. (2020). Open database analysis of scaling and spatio-temporal properties of power grid frequencies . *Nature Communications*, 11, 1.

Rydin Gorjão, L., Schäfer, B., Witthaut, D., and Beck, C. (2021). Spatio-temporal complexity of power-grid frequency fluctuations. *N. J. Phys.*, 23, 073016.

Schäfer, B., Beck, C., Aihara, K., Witthaut, D., and Timme, M. (2018). Non-gaussian power grid frequency fluctuations characterized by lévy-stable laws and superstatistics. *Nat. Energy*, 3, 119–126.

Schröder, M., Zhang, X., Wolter, J., and Timme, M. (2020). Dynamic perturbation spreading in networks.

IEEE Transactions on Network Science and Engineering, 7, 1019–1026.

Siami, M. and Motee, N. (2016). Fundamental limits and tradeoffs on disturbance propagation in linear dynamical networks. *IEEE Transactions on Automatic Control*, 61(12), 4055–4062.

Stephenson, K. and Zelen, M. (1989). Rethinking centrality: Methods and examples. *Social Networks*, 35, 460.

Tegling, E., Bamieh, B., and Gayme, D.F. (2015). The price of synchrony: Evaluating the resistive losses in synchronizing power networks. *IEEE Trans. Control Net. Syst.*, 2, 254–266.

Tumash, L., Olmi, S., and Schöll, E. (2019). Stability and control of power grids with diluted network topology. *Chaos*, 29, 123105.

Tyloo, M. and Jacquod, P. (2021). Primary control effort under fluctuating power generation in realistic high-voltage power networks. *IEEE Control Systems Letters*, 5, 929.

Tyloo, M., Pagnier, L., and Jacquod, P. (2019). The key player problem in complex oscillator networksand electric power grids: Resistance centralities identify local vulnerabilities. *Sci. Adv.*, 5, eaaw8359.

Tyloo, M. and Jacquod, P. (2019). Global robustness versus local vulnerabilities in complex synchronous networks. *Phys. Rev. E*, 100, 032303.

Ulbig, A., Borsche, T.S., and Andersson, G. (2014). Impact of low rotational inertia on power system stability and operation. *IFAC Proceedings Volumes*, 47(3), 7290–7297.

Wolff, M., Schmietendorf, K., Lind, P., Kamps, O., Peinke, J., and Maass, P. (2019). Heterogeneities in electricity grids strongly enhance non-gaussian features of frequency fluctuations under stochastic power input. *Chaos*, 29, 103149.

Xiao, W. and Gutman, I. (2003). Resistance distance and laplacian spectrum. *Theoretical Chemistry Accounts*, 110(4), 284.